

# Composition and Structure of Czochralski Silicon Implanted with $H_2^+$ and Annealed under Enhanced Hydrostatic Pressure

M. KULIK<sup>a</sup>, A.P. KOBZEV<sup>b</sup>, A. MISIUK<sup>c</sup>, W. WIERZCHOWSKI<sup>d</sup>, K. WIETESKA<sup>e</sup>  
AND J. BAK-MISIUK<sup>f</sup>

<sup>a</sup>Institute of Physics, Maria Curie-Skłodowska University, pl. Marii Curie-Skłodowskiej 1, 20-031 Lublin, Poland

<sup>b</sup>Joint Institute for Nuclear Research JINR, Joliot-Curie 6 st., 141980 Dubna, Moscow Region, Russia

<sup>c</sup>Institute of Electron Technology, al. Lotników 32/46, 02-668 Warsaw, Poland

<sup>d</sup>Institute of Electronic Materials Technology, 01-919 Warsaw, Poland

<sup>e</sup>Institute of Atomic Energy, 05-400 Otwock-Świerk, Poland

<sup>f</sup>Institute of Physics, Polish Academy of Sciences, al. Lotników 32/46, 02-668 Warsaw, Poland

Depth distribution of implanted species and microstructure of oxygen-containing Czochralski grown silicon (Cz-Si) implanted with light ions (such as  $H^+$ ) are strongly influenced by hydrostatic pressure applied during the post-implantation treatment. Composition and structure of Si:H prepared by implantation of Cz-Si with  $H_2^+$ ; fluence  $D = 1.7 \times 10^{17} \text{ cm}^{-2}$ , energy  $E = 50 \text{ keV}$  (projected range of  $H_2^+$ ,  $R_p(H) = 275 \text{ nm}$ ), processed at up to 923 K under Ar pressure up to 1.2 GPa for up to 10 h, were investigated by elastic recoil detection Rutherford backscattering methods and the depths distributions of implanted hydrogen and also carbon, oxygen and silicon in the near surface were determined for all samples. The defect structure of Si:H was also investigated by synchrotron diffraction topography at HASYLAB (Germany). High sensitivity to strain associated with small inclusions and dislocation loops was provided by monochromatic ( $\lambda = 0.1115 \text{ nm}$ ) beam topography. High resolution X-ray diffraction was also used.

PACS numbers: 61.72.U–, 61.72.uf, 66.10.C–, 61.80.Jh, 81.20.–n, 82.80.Yc, 85.40.–e

## 1. Introduction

Ion implantation is a technique widely used in the technology of electronic devices made on silicon [1, 2]. Recently, a growth of interest with implantation of hydrogen into silicon was observed. In some papers there were presented the studies of the diffusion process of hydrogen in amorphous Si after implantation [3] and formation of isolator structures in Si after implantation [4]. Hydrogen implantation has been often used to shear and transfer a thin silicon layer in implanted wafer onto a supporting wafer after bonding the two wafers together and subsequent annealing [5, 6]. This work is concerned on the investigations of distributions of hydrogen and concentration of oxygen and carbon in near surface layers of implanted Si after thermal annealing.

## 2. Experimental

(001) oriented polished Cz-Si wafers of 100 mm diameter and standard microelectronic quality were used in the described experiment.

Composition and structure of Si:H prepared by implantation of Cz-Si with  $H_2^+$ ; fluence  $D = 1.7 \times 10^{17} \text{ cm}^{-2}$ , energy  $E = 50 \text{ keV}$ , (projected range hydrogen,  $R_p(H) =$

275 nm), processed at 723 K and at 923 K under Ar pressure up to 1.2 GPa (high pressure, HP). HP was applied during annealing of Si:H up to 10 h. The depths profiles of hydrogen and the effects of diffusions were investigated by elastic recoil detection (ERD) and Rutherford backscattering spectrometry (RBS) methods. ERD and RBS measurements have been performed at room temperature. Both methods were simultaneously used in the study of implanted and annealed samples. The energy of exploring ions  $He^+$  ions was 2.297 MeV, the shuttering angle was  $\theta = 170^\circ$ , and the incidence angle of the ion beam on the studied surfaces equals  $\phi = 75^\circ$  in the RBS experiment. At the same time recoil hydrogen ions were collected through semi-conductive detector. The angle between the  $He^+$  beam and the direction of collected hydrogen was  $30^\circ$ .

The defect structure of Si:H was investigated by synchrotron diffraction topography at HASYLAB (Germany). X-ray (synchrotron) measurements were performed at room temperature.

The samples were systematically studied with various synchrotron topographic methods both in the white and monochromatic beam and by recording the local rocking curves.

The synchrotron X-ray white beam investigations were performed at the experimental station F1 including taking back-reflection section and projection topographs. In both cases a relatively low glancing angle 4–5° was used. In case of section topographs the beam was limited with a 5  $\mu\text{m}$  narrow slit.

The monochromatic beam investigation was performed in the 0.1115 nm radiation monochromatic beam. The angular setting enabled to reproduce a great part of the sample at the setting at the slope of the diffraction peak. The sizes of the probe beam used for recording of the local rocking curves were close to 50  $\mu\text{m}$   $\times$  100  $\mu\text{m}$ .

Similarly as in the case of our investigations of  $\text{A}^{\text{III}}\text{B}^{\text{V}}$  compounds implanted with hydrogen the rocking curves of the as implanted sample contained a series of additional interference maxima at the low angle tail of the rocking curve.

### 3. Results

In Fig. 1 there are presented the synchrotron rocking curves of the reference hydrogen implanted with  $\text{H}^+$  ions. The period of these maxima systematically increases toward the low angle, being the largest for the most left sample (Fig. 1a). The curve was analogous to the other analysed in the implantation with hydrogen and indicates the presence of a maximally strained buried layer located close to the maximum of the ion distribution. This maximum seems to be the common effect of interstitial hydrogen and the introduced complexes of point defects in the silicon matrix. A certain lifting of maxima in the middle part of the tail indicates the presence of strain caused by introduced point defects in the silicon matrix, analogously as in case of  $\text{A}^{\text{III}}\text{B}^{\text{V}}$  compounds [7, 8].

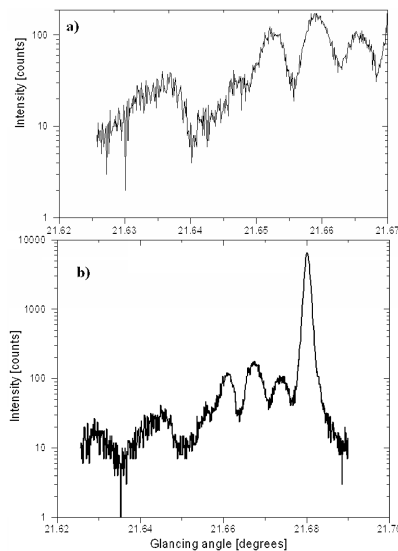


Fig. 1. The synchrotron rocking curve of the reference hydrogen implanted sample of Cz-Si. a) curve presenting the initial part of the tail with the interference maxima b) total curve.

It was found that the high temperature (HT) treatment (here 725 K and 923 K) leads to the process of strong decrease of the strain, probably also as the result of precipitation of hydrogen in complexes of silicon vacancies. That resulted in the complete vanishing of the interference maxima in the rocking curves. At the atmospheric pressure we observed formation of local exfoliation bubbles visible in section and projection topographs. These phenomena cause slight FWHM increase and lifting the tails of the rocking curve. The back-reflection section topographs usually helped the indication whether the distribution of the observed defects is of near-surface or volume character (Fig. 2).

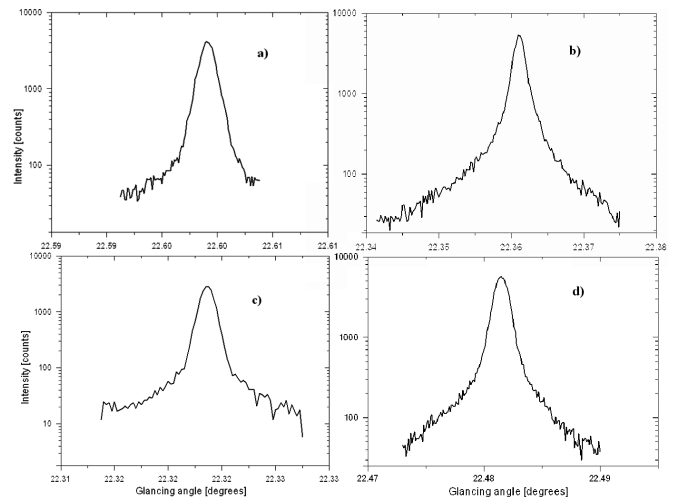


Fig. 2. The synchrotron rocking curve of sample of Cz-Si implanted with  $\text{H}^+$  ions: (a) annealed at 923 K at atmospheric pressure, (b) annealed at 723 K at  $12 \times 10^8$  Pa, (c) annealed at 923 K at atmospheric pressure, (d) annealed at 923 K at  $12 \times 10^8$  Pa.

The HP presence up to  $12 \times 10^8$  Pa moderated the process of exfoliation resulting in lower concentration of defects visible in the topography, as well in lower increase of FWHM, and in lower tails of the rocking curve. In this case the section back-reflection pattern revealed the pattern of the interference fringes characteristic for the bent silicon wafers of good crystallographic quality.

The synchrotron white beam section (upper) and projection (lower) topography of sample of Cz-Si implanted with hydrogen is presented in Fig. 3.

In Fig. 4 there is shown a typical RBS spectrum, collected for implanted Si. Two maxima were observed in RBS spectrum near the energy 0.6 MeV and 0.9 MeV. These peaks are connected with the scattered  $\alpha$  particles on the nucleons of carbon and oxygen atoms situated in the near surface layers of Si. On the basis of RBS and ERD measurements, depth profiles of the elements were determined. The simulated spectrum obtained with the help of SIMNRA computer code is in a good agreement with experimental results. It means that the applied model is consistent with reality.

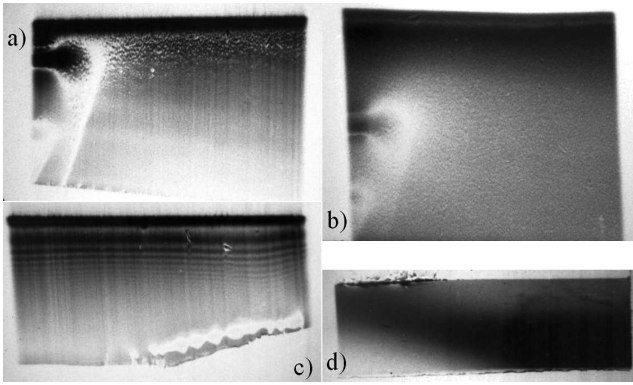


Fig. 3. The synchrotron white beam section a) and projection b) topography of sample of The synchrotron white beam section (a) and projection (b) topography of sample of Cz:Si  $H^+$  implanted, annealed at 923 K at atmospheric pressure, (c) annealed at 923 K pressure under  $12 \times 10^8$  Pa revealing the interference pattern characteristic for slightly bent silicon wafers of good perfection, (d) annealed at 923 K at pressure under  $12 \times 10^8$  Pa, confirming the lack of exfoliation bubbles.

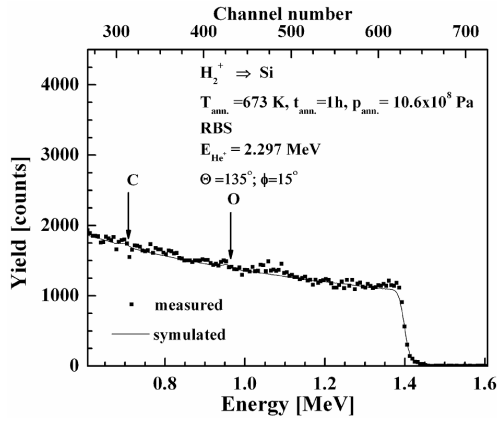


Fig. 4. The RBS spectrum measured for Cz-Si implanted with  $H^+$  fluence  $D = 1.7 \times 10^{17} \text{ cm}^{-2}$  and energy  $E = 50 \text{ keV}$ .

In Fig. 5 there are presented collected and simulated (by SIMNRA) ERD spectra for the all samples. It was noticed in Figs. 5a–d that the growth of the annealing temperature causes a shift of the spectra maxima to higher energies. This effect can be attributed to hydrogen diffusion to the surface. It was observed also that with the increase of the annealing time the hydrogen concentration decrease, and this effect can be explained by the loss of hydrogen atoms from the implanted layers during the process of thermal annealing. In Figs. 5a and c a shift of spectra to the lower energies with growing of annealing pressure is observed. This effect is connected with the process of diffusion of hydrogen into the depth of the samples. In Fig. 6 the results of determinations of the depth distributions of hydrogen in the implanted Si after thermal annealing are presented. It is observed

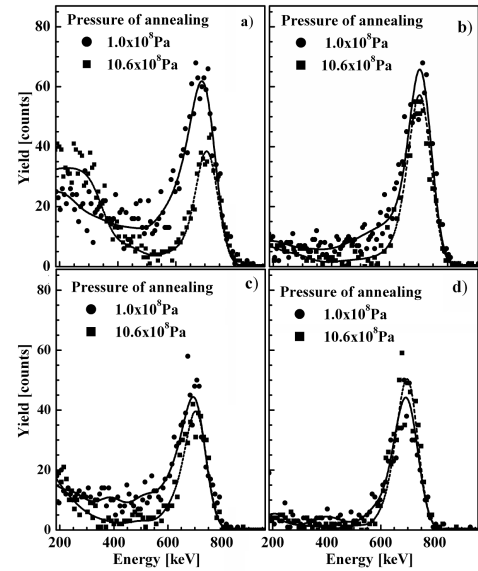


Fig. 5. ERD spectra measured for Si implanted with  $H^+$  fluence  $D = 1.7 \times 10^{17} \text{ cm}^{-2}$  and energy  $E = 50 \text{ keV}$ . Best fits (solid and dashed lines) were obtained for samples annealed at pressure  $1.0 \times 10^8 \text{ Pa}$  and  $10.6 \times 10^8 \text{ Pa}$ , respectively. The results are presented for samples annealed for 1.0 h at 723 K (a) and 923 K (b) and for 10.0 h at 723 K (c) and 923 K (d).

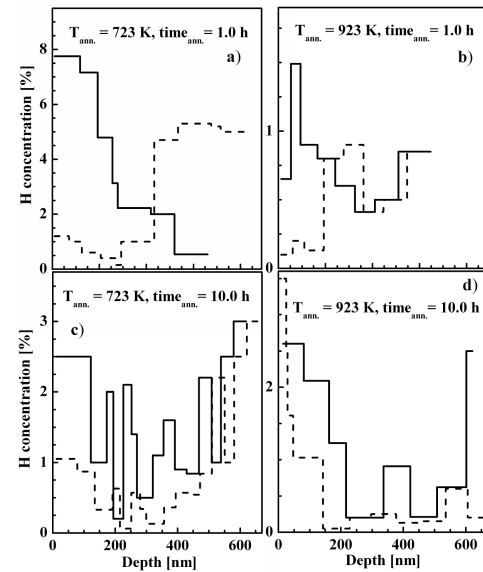


Fig. 6. The depth profiles distributions of hydrogen determined on the basis of ERD and RBS spectra measured for Si implanted with  $H^+$  fluence  $D = 1.7 \times 10^{17} \text{ cm}^{-2}$  and energy,  $E = 50 \text{ keV}$ . Depth profiles (solid and dashed lines) obtained for samples annealed at pressure  $1.0 \times 10^8 \text{ Pa}$  and  $10.6 \times 10^8 \text{ Pa}$ , respectively at different annealing times: 1 h and 10 h.

that together with the growth of the pressure during annealing the concentration of hydrogen increases in deeper regions of the sample.

It is found that the growth of the annealing time causes a decrease of the concentration of hydrogen in samples annealed at 723 K and we can observe also a diffusion process of hydrogen towards the surface in the Si implanted and annealed at 923 K samples.

#### 4. Conclusions

To summarize these studies, all parameters of annealing are very important in the process of hydrogen diffusion in implanted Si. The pressure at the annealing process plays a decisive role in the creation of the depth distribution of hydrogen and suitable profile could be obtained by changing the pressure.

#### Acknowledgments

This work was partly supported by the European Community Seventh Framework Programme (FP7/2007–2013) under grant no. 226716.

#### References

- [1] R. Kuroda, A. Teramoto, Y. Nakao, T. Suwa, M. Konda, R. Hasebe, X. Li, T. Isogai, H. Tanaka, S. Sugawa, T. Ohmi. *Jap. J. Appl. Phys. Part 2* **48**, 04C048 (2009).
- [2] N.G. Rudawski, K.S. Jones, S. Morarka, M.E. Law, R.G. Elliman, *J. Appl. Phys.* **105**, 081101 (2009).
- [3] B.C. Johnson, J.C. McCallum, A.J. Atanacio, K.E. Prince, *Appl. Phys. Lett.* **95**, 101911 (2009).
- [4] I.E. Tyschenko, A.B. Talochkin, E.M. Bagaev, A.G. Cherkov, V.P. Popov, A. Misiuk, R.A. Yankov, *J. Appl. Phys.* **102**, 074312 (2007).
- [5] A. Misiuk, A. Shalimov, B. Surma, J. Bak-Misiuk, A. Wnuk, *J. Alloys Comp.* **401**, 205 (2005).
- [6] A. Wolska, K. Lawniczak-Jablonska, M. Klepka, W.S. Walczak, A. Misiuk, *Phys. Rev. B* **75**, 113201 (2007).
- [7] W. Wierzchowski, K. Wieteska, A. Turowski, W. Graeff, G. Gawlik, *Vacuum* **63**, 767 (2001).
- [8] K. Wieteska, W. Wierzchowski, W. Graeff, G. Gawlik, *Phys. Status Solidi A* **203**, 227 (2006).